Paper ID
DRC1009

The 3rd TSME International Conference on Mechanical Engineering
October 2012, Chiang Rai

Control of a Two-Degree of Freedom Cable Driven Compound Joint System: Preliminary Results

Phongsaen Pitakwatchara

Department of Mechanical Engineering, Faculty of Engineering
Chulalongkorn University, Bangkok, THAILAND 10330
Email: phongsaen.p@chula.ac.th

Abstract

This is an ongoing work on the two-degree of freedom cable driven compound joint system. Construction of the prototype has been completed and currently the work on controlling this system has just begun. Here some preliminary results are reported. Namely, a simple Proportional-Derivative (PD) controller on the individual motor is designed and tuned based on the motor's model solely. Then, this same controller is applied to drive the compound joint system according to the desired motion. The resulting response from even such this simple controller is quite satisfactory, not surprisingly thanks to the well-designed of the system dynamics. Overall, the closed loop system is passively stable and hence can interact with the passive environment safely. Friction in the system induces the constant offset of the tracking task, however. For this purpose, two strategies, the supervisory correction command and the drift error correction control law, have been proposed. The latter approach leads to the Proportional-Integral-Derivative (PID) controller. A friendly graphical user interface (GUI) has been developed along with; allowing the user to specify his/her desired motion intuitively.

Keywords*:* PD controller, PID controller, GUI for motion control, cable driven robot

1. Introduction

Prior work of the author [1-3] reported the analysis and design of a two-degree of freedom (DOF) cable driven compound joint system. It is intended to be a study prototype of a cable-driven robotic system, in particular the anthropomorphic arm. At present, the prototype was constructed, as shown in Fig. 1. The system possesses two DOF, hence making the output linkage able to travel in the pitching and yawing directions. This motion grossly mimics the major rotations of the human shoulder joint. The travel range is approximately $\pm 65^{\circ}$ for each, hence with the output link length of 315 mm covering the working area of approximately 3,700 cm^2. Further details of the robot specifications are stated in [2, 3].

Preliminary work on control of the robot has been addressed in this work. Specifically, a simple controller on each motor is designed and tuned based on its model solely. Then these servo motors are equipped to the robot and used to drive the system according to the desired motion. In other words, the robot dynamics is not taken into consideration.

Section 2 explained the design of a simple Proportional-Derivative (PD) controller for the motor unit. Together with the gravity compensator, they form the simple controller for the robot. Modifications of this controller to solve the constant offset problem of the tracking task are presented in section 3, where the experimental verifications are shown along with. Development of a friendly graphical user interface (GUI) is mentioned in section 4. Finally, discussion of this preliminary work and future research direction are given in section 5.

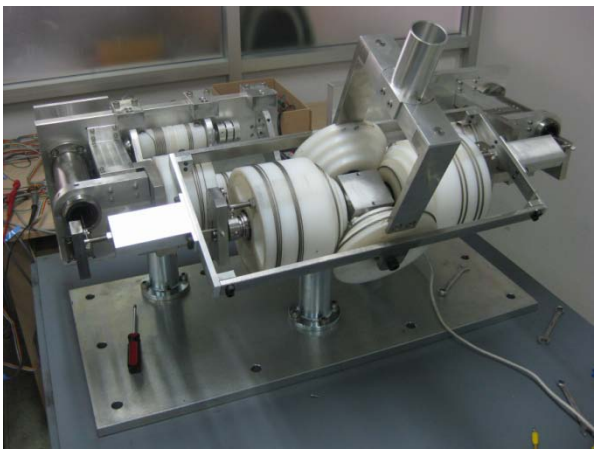

Fig. 1: Photo of the two DOF cable driven compound joint system

2. Simple Control of the Robot

2.1 Model of the DC motor

Motor may be viewed as the instrument which transforms the electrical power into the

mechanical power. Here the inertia effects and losses in both domains will be considered in its modeling. Referring to the DC motor schematic diagram in Fig. 2, R_e and I_e are the lumped resistance and inductance in the armature coil and R_m and I_m are the mechanical viscous friction and inertia of the rotor. κ is the motor torque constant. If the motor is operated under current mode, its dynamics is governed by the following equation

$$I_m\ddot{\theta} + R_m\dot{\theta} = \kappa i \qquad (1)$$

where i is the supplied current to the motor and θ is the rotor angle.

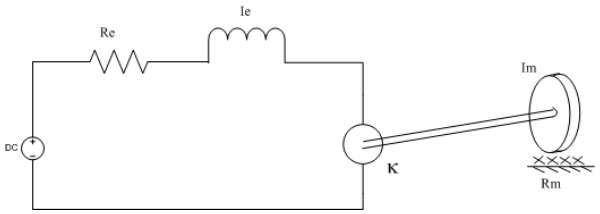

Fig. 2: Schematic diagram of the DC motor

2.2 A simple PD controller

The following PD control law

$$i = -\frac{1}{\kappa}\left[R_m'\dot{\theta} + K_d(\theta - \theta_d)\right] \qquad (2)$$

is proposed. Using this controller, the closed loop system equation becomes

$$I_m\ddot{\theta} + R_d\dot{\theta} + K_d(\theta - \theta_d) = 0 \qquad (3)$$

where $R_d = R_m + R_m'$ is the desired damping value and K_d the desired stiffness. It can be easily shown that this closed loop motor system has the globally asymptotically stable equilibrium point at $\theta = \theta_d$ and $\dot{\theta} = 0$.

From the motor's data sheet, $I_m = 13.8 \times 10^{-6}\ \text{kg}\cdot\text{m}^2$, $R_m = 4.14 \times 10^{-3}\ \text{Nm}\cdot\text{s/rad}$, and $\kappa = 60.3 \times 10^{-3}\ \text{Nm/A}$. If the value of R_m' and K_d are selected to be $1 \times 10^{-3}\ \text{Nm}\cdot\text{s/rad}$ and $1.43 \times 10^{-1}\ \text{Nm/rad}$, the closed loop motor system theoretically behaves according to the following second order linear ODE:

$$13.8 \times 10^{-6}\ddot{\theta} + 4.14 \times 10^{-3}\dot{\theta} + 1.43 \times 10^{-1}(\theta - \theta_d) = 0. \qquad (4)$$

Hence the closed loop system has the characteristics of $\omega_n = 16.2\ \text{Hz}$ and $\zeta = 1.83$, indicating a fast enough and well damped system.

The designed controller is implemented digitally on a desktop computer with Intel® Core™ 2 Quad processor. The control loop runs at the average speed of 1 kHz. For a given set point value, the cycloidal curve is used to generate a transitional profile which has smooth velocity to prevent the control saturation. If the set point A is required to be reached within T seconds, the motion profile θ during $0 \le t \le T$ is described by

$$\theta = \frac{A}{T}\left(t - \frac{\sin\frac{2\pi}{T}t}{\frac{2\pi}{T}}\right). \qquad (5)$$

2.3 Gravity torque and compensation

Mass and inertia of the robot's parts account for the gravity force, which, in turn, induces the gravity torque. A convenient way to derive such term is to determine it from the potential energy. Referring to the parameters and bond graph model of the system [2, 3], the total potential energy V_r of the robot can be written as

$$V_r = -m_p g r_{z_p} s_p - m_{py} g r_{z_{py}} s_p c_y, \qquad (6)$$

where m_p and m_{py} are the aggregated mass of the parts that undergo the pure pitching motion and the compound pitching and yawing motion, respectively. r_{z_p} and $r_{z_{py}}$ are the distance of the compound center of gravity of the parts that undergo the pure pitching motion and the compound pitching and yawing motion, measured from the center point of rotation.

Gravity torque may be compensated by the motor torque. This, however, requires the suitable motor sizing, otherwise motor saturation will happen. Additionally, this approach assumes proper operation of the motors. Violation might occur due to the power blackout or the malfunction of the control system. The robot motion will then be overruled by the gravity effect, which may cause the accident that cannot be compromised for the service robots.

Therefore, this robot is equipped with the patented pending spring-based counter-balancing mechanism [4]. This mechanism theoretically generates the torque, based on the current posture of the robot, which is oppositely equal to the gravity torque. As a result, no motor torque is required for the gravity compensation and hence the robot is inherently safe.

Unfortunately, mechanical compensation of the gravity torque is not perfect as desired. This is due mainly to the mismatch between the designed spring stiffness and the actual one obtained from the available off-the-shelf spring. Therefore, a small motor torque is needed in addition to completely cancel the gravity torque. This torque is associated with the potential energy V_m that makes the total potential of the system be constant. Mathematically,

$$V_m = -V_r - V_c, \qquad (7)$$

where V_c is the potential energy of the counter-balancing mechanism. Development of the required motor torque expression is rather lengthy and shall be excluded from the paper. With this

gravity compensation system, the PD controller will be responsible for the tracking of the desired motion solely.

2.4 Simple control of the robot

Two of the controlled motors, as described in section 2.2, and the gravity compensation system are now used for positioning control of the robot. As for the initial work, the controlled motors acting as the servo motors, are equipped to the robot. Then, the inverse kinematics will be performed to transform the coordinates of the set point specified in the task space (pitch and yaw angles, θ_p and θ_y) to the coordinates in the joint space (two motor angles, θ_{w1_l} and θ_{w1_r}). Particularly,

$$\begin{bmatrix}\theta_{w1_l}\\ \theta_{w1_r}\end{bmatrix} = \begin{bmatrix}9 & -9\\ 9 & 9\end{bmatrix}\begin{bmatrix}\theta_p\\ \theta_y\end{bmatrix}, \qquad (8)$$

provided the initial angles are all reset to zero. These motor angles set point are regarded as the desired angle θ_d for the motor controller. In other words, the robot dynamics is not taken into consideration.

Figure 3 displays the response of the controlled system to a sequence of pitch and yaw set points; that is, $(0°, 0°)$, $(10°, 0°)$, $(20°, 0°)$, $(10°, 0°)$, $(0°, 0°)$, $(-10°, 0°)$, $(-20°, 0°)$, $(-10°, 0°)$, $(0°, 0°)$, $(0°, 10°)$, $(0°, 20°)$, $(0°, 10°)$, $(0°, 0°)$, $(0°, -10°)$, $(0°, -20°)$, $(0°, -10°)$, and $(0°, 0°)$ are given to the controller manually with enough settle time interval for each of them. It is observed that the response tracks the reference quite well, but with the exception of constant steady state error (less than 2°) due to some imperfect cancellation of the gravity torque and the underestimated stiction in the system. Overall, the closed loop system is passively stable and hence can interact with the environment safely.

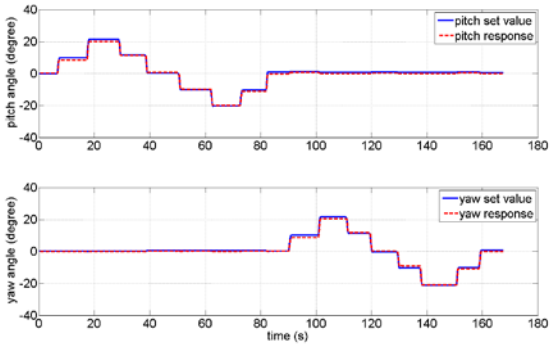

Fig. 3: Response of the robot motion
to a sequence of pitch and yaw set points
under a simple PD controller

3. Controller Modification

Simple PD controller does not respond to the zero-order steady state error. To correct this problem, two strategies are proposed.

3.1 Supervisory correction command

For the previous controller, single cycloidal step is used to generate the desired motion profile. However, fraction of the associated supplied energy must be given to the compliance and resistance effects of the gravity and friction. Therefore, the available energy to drive the robot is less than what has been expected, which causes the mismatch between the actual and the desired position. A simple notion of providing extra amount of energy to bring the robot to the desired position should solve this problem.

The scheme for the first approach is as follow. After the cycloidal motion profile is supplied for a certain time where the system may be assumed to be in the equilibrium, a supervisory program monitors the position error. The mismatch will then be used as a new relative set point A to generate an additional cycloidal step. In other words, a high level of the controller is employed to generate appropriate command to the low level controller. The use of such a simple strategy can be found in biological livings. Blind people use haptic queue to help manipulating the objects successfully, for example.

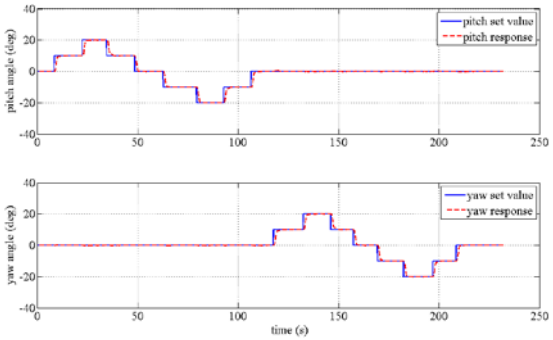

Fig. 4: Response of the robot motion
using the simple PD controller
and the simple supervisory controller

Figure 4 shows the response of the system under the simple PD controller with the adjunct supervisory controller. In this experiment, parameter T of the motion profile has been set to 2 seconds, which is the same as the update time of the supervisory controller. Position error of the robot becomes zero after one or two corrective pulse. Again, since the controller and the robot are passive systems, therefore the interconnecting closed loop is also passive system.

3.2 Drift error correction control law

The second approach continually monitors the position error, which is then used to modify the original control law for the purpose of zero steady state error [5].

Let $d(t) = \theta(t) - \theta_d(t)$ denotes the tracking error. Therefore the original tracking PD control law $\hat{u}$ may be written as

$$\hat{u} = -R_m' \dot{d} - K_d d. \quad (9)$$

This control law must be corrected by $\Delta u(t)$, resulting in a new control law

$$u(t) = \hat{u}(t) + \Delta u(t). \quad (10)$$

At steady state, Eq. (9) reduces to

$$d(t) = -\frac{\hat{u}(t)}{K_d}. \quad (11)$$

The control value at steady state should be unchanged, i.e. $\dot{u}(t) = 0$. Differentiating Eq. (11) and applying this fact result in the following relation;

$$\dot{d}(t) = \frac{\Delta\dot{u}(t)}{K_d}. \quad (12)$$

For the error $d(t)$ to be zero asymptotically,

$$\Delta\dot{u}(t) = -\lambda K_d d(t) \quad (13)$$

should be applied. Integrating Eq. (13) to obtain the corrective term as

$$\Delta u(t) = \lambda K_d \int_0^t (\theta_d - \theta) d\tau. \quad (14)$$

Therefore the modified controller is

$$u = R_m'(\dot{\theta}_d - \dot{\theta}) + K_d(\theta_d - \theta) + \lambda K_d \int_0^t (\theta_d - \theta) d\tau, \quad (15)$$

which is actually a PID controller that employs the integrator to provide the constant control input in solving the steady state error problem. Nevertheless, it should be mentioned that the PID controller itself is not passive, which makes the closed loop less stable than the PD one.

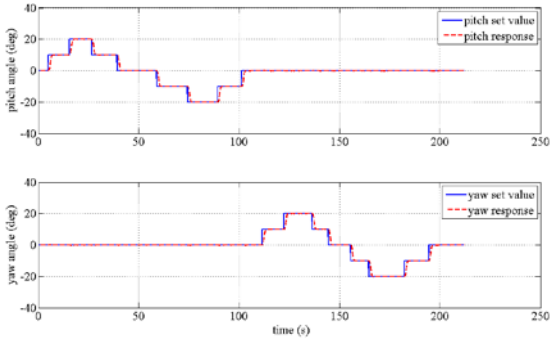

Fig. 5: Response of the robot motion using the PID controller

Previous experiment is now re-executed with the PID controller. With the value of the integral gain of 1.43×10^{-1} Nm/rad · s, the response of the system is depicted in Fig. 5. Without the external interacting force to the robot, the response is cleaner and faster compared to using the supervisory correction command.

4. GUI for the Motion Command

A friendly graphical user interface (GUI) has been developed to allow the user in specifying his/her desired motion intuitively. Since the end effector of the robot, i.e. the end tip of the output linkage, is constrained to be on the spherical surface, the user should be allowed to specify the robot motion only on the virtual spherical surface as well. For this reason, a spherical workspace is drawn on the two dimensional monitor, as shown in Fig. 6. This picture corresponds to the front view of the robot.

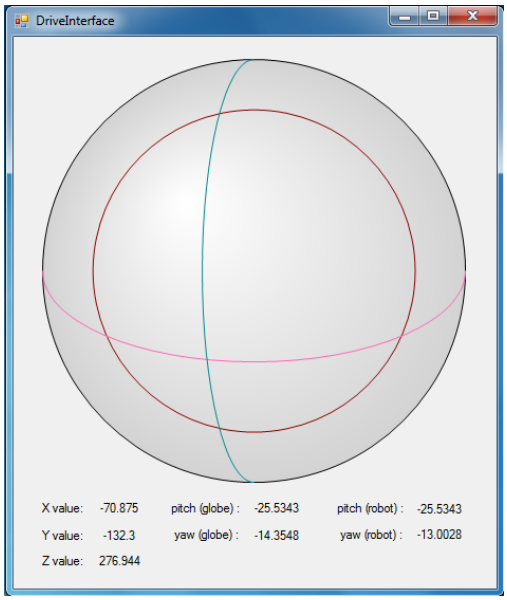

Fig. 6: A snapshot of the GUI for specifying the desired motion to the robot

The user indicates the desired motion by moving the mouse over the workspace. The program will then calculate the corresponding pitch and yaw angles of the differential joint from the x and y coordinates of the cursor as followed. Consider Fig. 7 which shows the top, front, and right side view of the workspace with its reference frame. With the known output link length, r, the z coordinate of the end effector will be

$$z = \sqrt{r^2 - x^2 - y^2}. \quad (16)$$

Pitch angle of the robot may now be calculated simply by

$$\theta_p = \tan^{-1}\left(\frac{y}{z}\right). \quad (17)$$

To calculate the yaw angle, it must be viewed along the y_r axis, which is moving according to

the changing pitch angle. See Fig. 7. In this view, the output link will always be seen as a true line. Therefore, the yaw angle can be calculated by

$$\theta_y = \sin^{-1}\left(\frac{x}{r}\right). \quad (18)$$

Additionally, the latitudinal and longitudinal curves of the current position are drawn in the GUI to provide the visual appearance of moving over the spherical surface. These curves can be constructed from the associated latitude and longitude angles, which, referring to Fig. 7, may be calculated from the coordinates of the point as

$$\theta_{lat} = \tan^{-1}\left(\frac{y}{z}\right), \quad (19)$$

$$\theta_{long} = \tan^{-1}\left(\frac{x}{z}\right). \quad (20)$$

Updated numerical values of these three coordinates are displayed in the bottom of the interface.

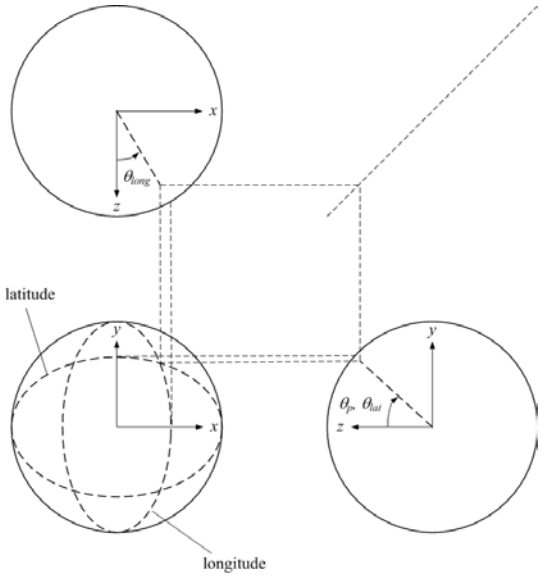

Fig. 7: Geometry for coordinate transformation of the robot

An experiment of the robot tracking task using the PID and the gravity compensation controller with the reference trajectory specified in real time from the user through the developed GUI is performed. Protocol of this experiment are as followed. The robot starts from rest at the middle point of the workspace. The user then moves the cursor horizontally to the right until the limiting brown circle is reached. The GUI will prevent any cursor movement that exceeds the limit. In effect, this is the soft limit of the robot.

After that, the user manipulates the cursor in the manner that it tracks the boundary of the limit in the counterclockwise direction for one round. Next the user moves the cursor horizontally to the left until the limit is reached again, at the left hand side for this time. In turn, the user manipulates the cursor in the manner that it tracks the boundary of the limit in the clockwise direction for one round. Finally the user moves the cursor horizontally to the right until it reaches the home position.

Plots of the reference and the response in the robot's pitch and yaw coordinates are depicted in Fig. 8. Tracking result is satisfactory for such a simple controller. An observable tracking delay of about 0.5 second is due to the tracking velocity limit set indirectly via the settling time of the updated point-to-point motion.

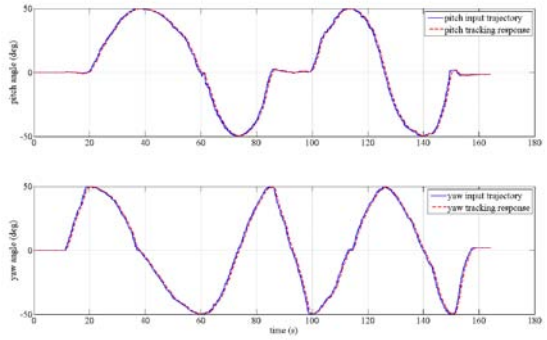

Fig. 8: Tracking response of the robot using the PID controller and gravity compensator

5. Discussions and Conclusions

In this paper, preliminary control of a two DOF cable driven robot using a simple PD and PID control laws are presented. Gravity compensation is conducted mainly by the counter-balancing mechanism. The remainder is taken care by the motor effort. Overall response of the system is fairly good. The robot can follow the specified trajectory closely.

The developed control law is based solely on the motor's dynamics. In particular, knowledge of the robot dynamics has not been exploited in designing the controller. This simplification will adversely affect the response of more demanding tasks. Since the power from the motors is transmitted mechanically through the cables and pulleys that inherently possess the compliance characteristics [1, 2], the robot naturally will exhibit a degree of vibration in its motion. This phenomenon may be evident during rapid movement, which causes the overshoot and the recurring oscillation. Worse yet, ignorance of flexibility in the robot may result in the unstable system.

Therefore in the next phase, a rigorous investigation on designing the controller based on the flexible robot model will be pursued. Moreover, since the robot is intended to perform collaborative tasks with humans, the controller should be designed based on the interaction control framework. Topics on determining the suitable impedance, the utilization of the inherent joint flexibility, and the impedance alteration are among our interest.

6. Acknowledgement

This work is generously supported by grants from the Engineering Faculty Research Funding, A Centennial Chulalongkorn University Research Funding, and the ISUZU Research Foundation.

7. References

[1] Pitakwatchara, P. (2010). Analysis and Modeling of the Cable-Pulley Power Transmission System in Robot, paper presented in *The 2010 IASTED International Conference on Robotics (ROBO 2010)*, Phuket, Thailand.

[2] Pitakwatchara, P. (2011). Design and Analysis of a Two-Degree of Freedom Cable Driven Compound Joint System, paper presented in *The Second TSME International Conference on Mechanical Engineering (TSME-ICOME)*, Krabi, Thailand.

[3] Pitakwatchara, P. (2012). A Two-Degree of Freedom Cable Driven Compound Joint System, Research Report No. 207-ME-2553, Faculty Research Fund, Faculty of Engineering, Chulalongkorn University.

[4] Pitakwatchara, P. (2012). Spring-Cable Counter-Balancing System for Pitch-Yaw Compound Joint Mechanism, Thailand Patent Pending, Patent Application No. 1201002792.

[5] Niemeyer, G. and Slotine, J. (2004). Telemanipulation with Time Delays, *International Journal of Robotics Research*, Vol. 23 (9), pp. 873-890.